Available online at www.sciencedirect.com
SCIENCE DIRECT®
Precambrian Research 137 (2005) 253–272
Precambrian Research
www.elsevier.com/locate/precamres

Black shales, organic matter, ore genesis and hydrocarbon generation in the Paleoproterozoic Franceville Series, Gabon

David J. Mossman [a,*], François Gauthier-Lafaye [b,1], Simon E. Jackson [c,2]

[a] *Department of Geography, Mount Allison University, 144 Main St. Sackville, NB, Canada E4L 1A7*
[b] *Ecole et Observatoire des Sciences de la Terre, Centre National de la Recherche Scientifique, 1 rue Blessig, 67084 Strasbourg, France*
[c] *GEMOC National Key Centre, School of Earth Sciences, Macquarie University, Sydney, NSW, Australia*

Accepted 1 March 2005

Abstract

The 2.1 Ga old FB Formation of the Franceville Series, southeastern Gabon, contains one of the greatest accumulations of organic carbon of its age. The weakly metamorphosed, dominantly pelitic, FB Formation ranges in thickness from 400 to 1000 m, covers over 35,000 km^2, and consists of about 80% marine shale with 0.5 to over 10% total organic carbon. Analyses show that, compared with black shale standard SD O-met, the average FB Formation black shale is enriched only in Au, Ag, Ba, and Cr. General paucities in U and Mn represent negative anomalies in this area of world class U and Mn deposits. However, detailed geochemical profiles of the lower FB Formation show that Fe/Mn ratios increase upwards from the base of the formation. At least locally, Mn build-up in the sedimentary column may be linked to increased oxidation potential caused by photosynthesis. The abundance of decomposing organic matter also played a key role in further concentrating Mn in carbonate protore during early diagenesis. The enrichment process continues today on a spectacular scale by lateritization.

Genesis of the uranium ores in the area is closely linked to the burial history and the maturation of organic matter in black shales near the base of the Franceville Series. The presence in these rocks of diverse fossil remains, including a Gunflint-type association of stromatolites and microfossils, various planktonic species of Gunflintian age, and abundant carbonized microbial-like forms, provides the link to genesis of liquid bitumens in the Franceville Series. Prolific amounts of liquid hydrocarbon, the remnants of which have since solidified, were generated through the "oil window", opened during burial of the FB Formation ca. 2.0 Ga ago. The coincidence of uranium-bearing aqueous solutions with the main interval of hydrocarbon migration led to the localization of uranium ores in petroleum-type structural traps. Some of the richer uranium deposits served as loci for the development of the Oklo natural nuclear fission reactors. Analysis by LA-ICP-MS of mineral-free portions of solid bitumens,

* Corresponding author. Tel.: +1 506 364 2312; fax: +1 506 364 2625.
E-mail addresses: dmossman@mta.ca (D.J. Mossman), gauthier@illite.u-strasbg.fr (F. Gauthier-Lafaye), sijackso@laurel.ocs.mq.edu.au (S.E. Jackson).
[1] Tel.: +33 88 35 8500; fax: +33 88 36 7235.
[2] Tel.: +61 2 9850 8368; fax: +61 2 9850 6904.

0301-9268/$ – see front matter
doi:10.1016/j.precamres.2005.03.005

derived from the black shales, confirms the presence of various metals including Ba, V, Zn, and U (possibly as organometallic complexes) and serves to elucidate evolutionary pathways of bitumen and particular metal associations.

Keywords: Black shales; Organic matter; Geochemistry; Paleoproterozoic; Gabon

1. Introduction

The 2.1 Ga old black shales of the Franceville Series, Republic of Gabon (Fig. 1) rank as one of the major Precambrian accumulations of organic matter. In size, the only closely comparable Proterozoic accumulation of organic matter is shungite from the Jatulian Series of Russian Karelia (see McKirdy and Imbus, 1992). In Gabon, uranium ores occur within quartzose sandstones at the top of the FA Formation directly below black shales near the base of the series. Manganese ore occurs in the overlying, dominantly pelitic FB Formation (Cortial et al., 1990), which ranges from 400 m to more than 1000 m thick and extends over 35,000 km^2. Comprised of 80% marine shale, the total organic carbon content (TOC) of the FB Formation ranges from

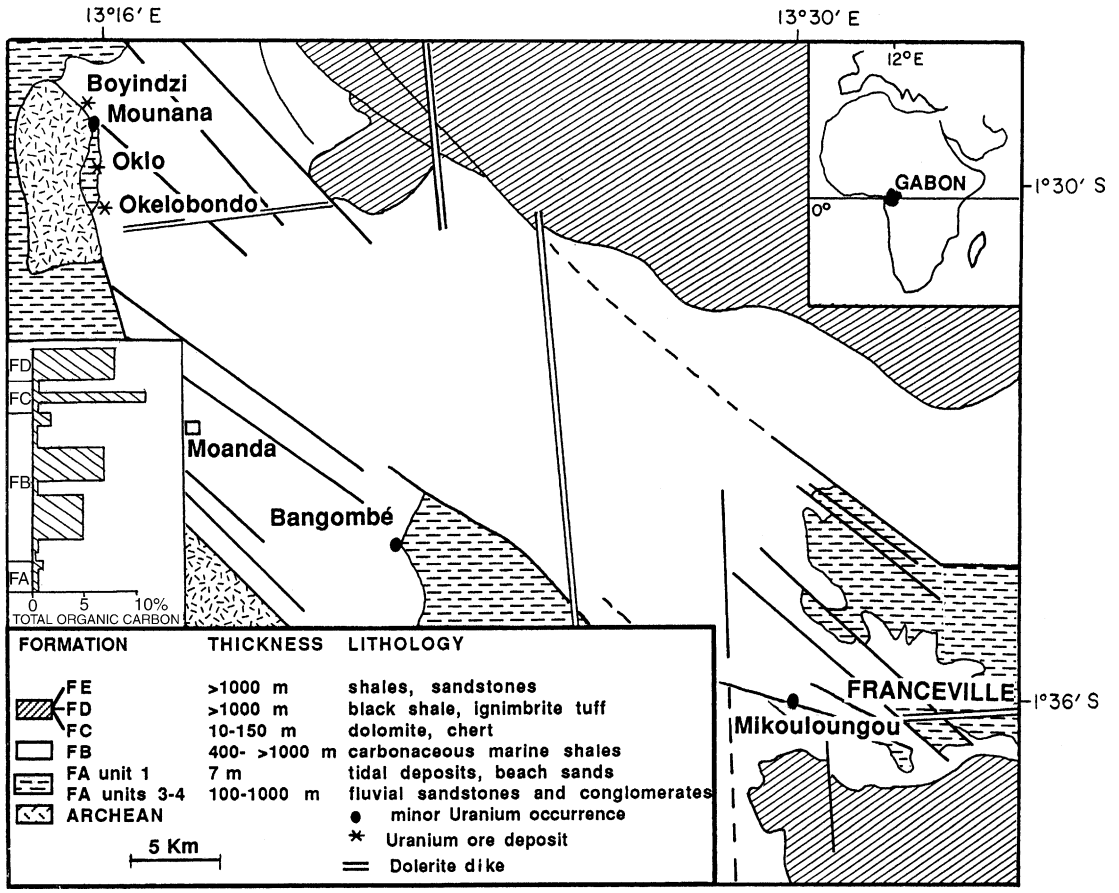

Fig. 1. Index map showing location of Oklo, Okelobondo, Moanda, Bangombe and Mikouloungou with respect to the general geology of the Paleoproterozoic Franceville Series (after Mossman et al., 1998). For a detailed stratigraphic section of the Franceville Series see Gauthier-Lafaye and Weber (1989).

0.5% to 15% (Gauthier-Lafaye and Weber, 1989). Results of detailed petrographic analysis of the organic matter indicates that a meta-anthracite grade (equivalent to lower greenschist facies of metamorphism) of maturation has been reached (Alpern, 1978; Cortial et al., 1990; Mossman et al., 1993).

Well-preserved fossil microbial assemblages occur in cherty stromatolites of the Franceville Group (Amard and Bertrand-Sarfati, 1997) and abundant microbial forms are present in the FB Formation black shales (Weber, 1968; Cortial et al., 1990; Mossman, 2001). According to Weber (1997) and Bertrand-Sarfati and Potin (1994), the decomposition of organic matter played a significant role during early diagenesis in the origin of the rich manganese ore deposits of the Franceville Series.

Following deposition and early diagenesis, organic matter (kerogen) of the FB Formation sourced prolific amounts of liquid petroleum, the remnants of which are now preserved as solid bitumens in the FA and FB formations (Mossman, 1998, 2001). The coincidence of uranium-bearing aqueous solutions with the main interval of petroleum migration led to the localization of the Oklo uranium ores in petroleum-type structural traps in the FA Formation ca. 1.968 Ga ago (Gauthier-Lafaye, 1986; Gauthier-Lafaye and Weber, 1981, 1989). Some of these structural traps served as loci for the development of 15 nuclear fission reactors at Oklo (Gauthier-Lafaye et al., 1996). Thus it appears that organic matter (kerogen and bitumen) played significant and diverse roles in the formation and evolution not only of the Franceville Series, but in associated processes of metal migration and concentration. There are clear indications too, that bitumen helped constrain the migration of fission products and radiogenic nuclides from the zones surrounding the nuclear fission reactors of Oklo. In this latter case bitumen geochemistry invites close attention from the perspective of anthropogenic nuclear waste containment issues.

Kerogen is an autochthonous solid polymer-like organic material, which does not migrate following deposition, whereas (solid) bitumen is an allochthonous organic solid that was at one time a viscous liquid (Mossman et al., 1993). Accepting these definitions, and given the abundance of kerogen and (derivative) bitumens in the Franceville Series, and the affinity of organic matter for certain metals (Disnar and Sureau, 1989; Quinby-Hunt and Wilde, 1991; Parnell et al., 1993; Leventhal and Giordano, 2000), the geochemistry of organic matter becomes a matter deserving close study. Here, with a perspective on the nature and origin of organic matter in the Franceville Series, the case for prolific hydrocarbon generation is assessed and the geochemistry of the black shales and derivative bitumens in these Paleoproterozoic sediments is examined.

2. Organic matter of the FB Formation

Several types of organic matter are documented from the sedimentary rocks of the Franceville Series. Alpern (1978) described kerogen (which he compared to boghead coal), two generations of bitumen, and a coke. A total of eight different types of carbonaceous substances (two kerogens, six solid bitumens) have been identified in the black shales and in the uranium ores and the fossil nuclear fission reactors (Jackson and Mossman, 1999; Mossman et al., 2001). Precursors to these various carbonaceous substances are cyanobacterial remnants in the FB Formation (Cortial, 1985; Cortial et al., 1990; Mossman et al., 1993; Mossman, 2001).

There is little doubt that microbes played a key role in contributing to the present high total organic carbon (TOC) content of the FB Formation and related sedimentary rocks. According to Amard and Bertrand-Sarfati (1997), the FB Formation and associated overlying units all contain a Gunflint-type association of stromatolites and microfossils; among the microfossils, at least one species (*Archaeoellipsoides*) is identified as planktonic. Microbial forms with ultralamellar structure are also widely present; for example, forms resembling sulfate-reducing bacteria are especially abundant in the so-called ‘coal’ at Mikouloungou (Mossman, 2001).

During pioneering studies of the Franceville Series, Weber (1968) recorded many curious microscopic forms associated with the manganese ore deposits, although he hesitated to commit to their identification as microfossils (F. Weber, personal communication). Many of these forms range from 20 to 30 μm in maximum diameter (Fig. 2), far larger than prokaryote cells according to the current view (de Duve, 1996). Detailed study of these particular forms has yet to be undertaken. However, the preservation of molecular fossils derived from biomarkers in 2.7 Ga old sediments

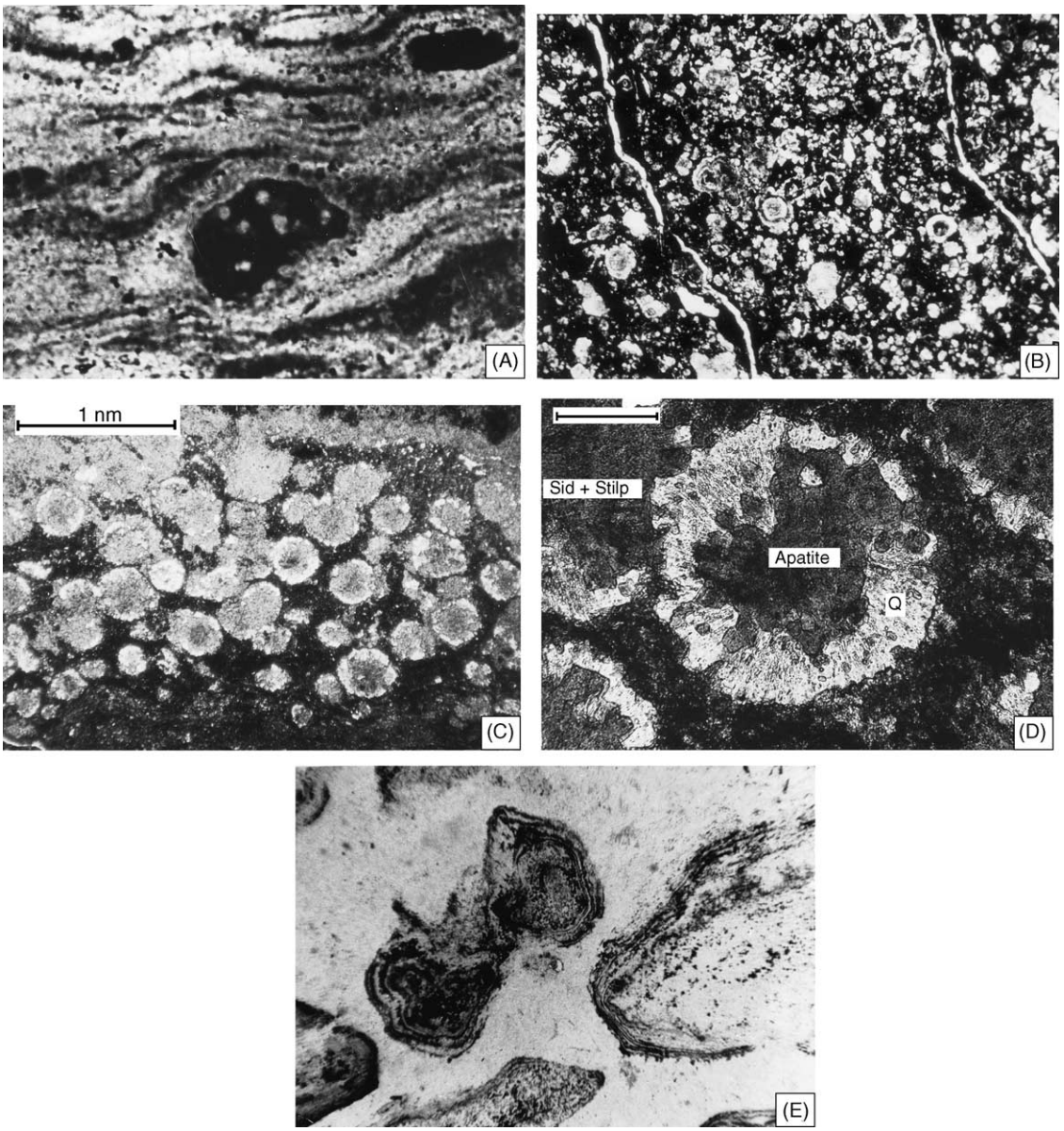

Fig. 2. Photomicrographs illustrating selected microbial forms from various types of the FB Formation. (A) Microstromatolites in Mikouloungou "coal". Sample ML 6-69. Field of view = 600 μm. (B) Pseudoolitic microfossils in chert from protore near the Moanda manganese mine, Bangombe Plateau (BA COMILOG bore hole). Sample RTM 488-L. Field of view = 600 μm. (C) Pseudoolitic structure preserved in chert in FB black shales on the Okouma Plateau immediately below the manganese ore horizon. Sample Ech 232-1. For detailed description see Weber (1968, p. 201, plate XII-6). Scale bar = 1 mm. (D) Detail of (C) reveals apatite at the center of the spherules, rimmed by quartz, and enclosed within a matrix of siderite and stilpnomelane. Scale bar = 100 μm. (E) Microstromatolites preserved as carbonaceous substances and pyrite in chert near manganiferous protore of the FB Formation. Location: Vieux M'Vengue. Sample FW 73-LNX. Field of view = 2.4 mm.

(Brocks et al., 1999) makes it highly probable that multicellular organisms were in existence well before deposition of the Franceville Series. In the mixed carbonate [(Mn, Ca, Mg) (CO_3)] phase protore of the (Moanda) manganese deposit, manganese enrichment was intimately associated with early diagenesis of stromatolites (Azzibrouch-Azziley, 1986; Bertrand-Sarfati and Potin, 1994, p. 353, Fig. 16; Weber, 1973, 1997). Weber (1997, p. 108) has shown that the decomposition of abundant organic matter promoted the dissolution of Mn from protore during early diagenesis, concentrating it at the top of the FB Formation. There are clear indications too (see below) that living organisms probably played a very important part in bringing about a relative concentration of manganese in the first instance.

3. Hydrocarbon genesis ca. 2 Ga ago

The main episode of hydrocarbon generation and primary migration in the Franceville Series occurred during burial and thermal maturation of organic matter in the black shales. According to Gauthier-Lafaye and Weber (1989) and Mossman et al. (2001), carbon isotopic data support the concept that organic matter in the FB Formation black shales sourced petroleum liquids, since transformed into solid bitumen in the FB and (underlying) FA formations. The latter formation hosts the uranium ores of Gabon. This came about as a result of reduction reactions promoted by the confluence of liquid hydrocarbons and uranium-bearing aqueous solutions as detailed by Gauthier-Lafaye and Weber (1989) and by Nagy et al. (1991).

The existence and persistence of Precambrian oil is no longer cause for great surprise (Buick et al., 1998; Grantham et al., 1988; Rasmussen and Buick, 2000). What is perhaps more remarkable is the amount of oil that was generated early in the geologic record. As a prime example, consider the initial potential of the FB Formation of the Franceville Series. According to Tissot and Welte (1984), a minimum of 0.4–1.4% TOC generally is considered essential for the transformation and development of economic amounts of hydrocarbon. Hydrocarbon values in the recent sediments of coastal basins, continental shelf, and open marine basins, range from 20 to 100 ppm (dry weight basis of rock); extractable hydrocarbon (bitumen) tends to be higher in ancient shales. Hunt (1995) estimates 100–300 ppm extractable hydrocarbon for ancient shales, and considers 1% TOC "... a reasonable cutoff for oil source rocks, and 0.5% for gas source rocks". Likewise, Tissot and Welte (1984) consider 1% TOC as the minimum value for effective hydrocarbon generation and expulsion from oil-prone organic matter.

Starting with a primordial biomass, precursor to the evolution of the type I kerogen (Mossman et al., 1993) that is preserved in the FB Formation black shales, a conservative estimate of the amount of liquid hydrocarbon can be made. Further considerations include:

(1) The essentially unoxidized condition of the black shales.
(2) The 35,000 km^2 areal extent of the black shales.
(3) Their thickness: 400–1000 m.
(4) The present TOC: 0.5 to about 10% or more, which prior to diagenesis/alteration would have been at least 10% higher according to Arthur and Sageman (1994).

Choosing a minimum value of 2% TOC with 200 ppm extractable hydrocarbon, an area of 30,000 km^2, and the minimum thickness of 400 m, yields 12×10^{12} m^3 of source rock, one cubic meter of which will supply in excess of 1 l of petroleum. This is a conservative estimate of the original petroleum potential of the FB Formation. It translates to 12×10^9 m^3, or about 84×10^9 US barrels of petroleum, comparable to a modern supergiant oilfield.

4. Analytical methods

Results as reported in Tables 2–4 were obtained following dissolution in HF: shales, dolomites and cherts – major elements by UV Spectrometry; sandstones – major and trace elements by atomic absorption. For uranium, spectrofluorimetry was employed for concentrations <100 ppm. Detection limits were as follows: U: 0.5 ppm; Cu, Ag, Mo and Ga: 5 ppm; Pb, Zn, Ba, Bi, Sn, B, V, Ni, Co, Sr, Ge, Be and Li: 10 ppm; La: 20 ppm; As, Sb and Mn: 50 ppm; Zr: 100 ppm. Precision ±3% for major elements, ±10% for trace elements.

5. Geochemistry of the black shales

The FB Formation black shales fit the widely accepted standard definition of ". . . a dark-colored (grey or black) fine-grained (silt sized or finer), laminated sedimentary rock that generally is argillaceous and contains appreciable carbon (>0.5 wt.%)" (Huyck, 1990). According to Stribrny and Urban (1989) nomenclature and classification of fine-grained sedimentary rocks in the "black shales series", the Francevillian black shale samples are organic-rich pelites.

Prior to Mossman et al. (1995, 1998) reports on the geochemistry of the FB Formation black shales overlying the fossil nuclear fission reactors of Oklo, very little geochemical work had been conducted on these rocks. In review, Mossman et al. (1998) showed that the FB Formation black shale is not notably metalliferous (see analysis of AOK, Table 1), with Cr, Au, Ag and Ba only slightly enriched compared to the standard metalliferous shale SDO-1. The chondrite-normalized REE diagram of these rocks strongly resembles that of greywacke-shale turbidites of Archean greenstone belts. Apart from a paucity of REE compared to various black shale standards, geochemical variations observed among the black shale samples include enrichment in K, Ba, Cr and Ag in the lowermost samples in the black shale sequence, and the presence of a bleached zone (so-called green pelites) largely depleted of organic carbon at the base of the FB Formation. Mossman et al. (ibid) speculated whether volcano-sedimentary rocks and associated ophiolitic intrusions, well developed in the FB Formation north of the Franceville Basin (Weber, 1968), might have caused hydrothermal alteration at the base of the black shale sequence. However, it is more likely that the green pelites resulted from the alteration by oxidizing fluids during early diagenesis, perhaps during the uranium mineralization event. The phenomenon is related to the oxidation stage of the overall FA sandstones throughout the Franceville Basin.

Table 1 summarizes the geochemistry of average black shale of the FB Formation (termed "AOK" by Mossman et al., 1998) and compares it with the averages of two other black shales (the Alum Shale and the Mecca Quarry Shale) and with the SDO-1 standard. It is evident from these average values, as indicated by Leventhal (1998), that different black shales are indeed enriched in different metals. As Desborough et al. (1976) also observed, for reasons that are not always clear, metal-poor black shales may occur despite high organic matter productivity and (or) preservation. Black shales of the Paleoproterozoic Franceville Series FB Formation seem to represent a case in point. However, black shale geochemistry in the vicinity of the manganese mines near Moanda provides a most interesting contrast with AOK.

The new data, relative to the shales in the vicinity of the manganese mines, are from Azzibrouch-Azziley (1986). These samples are from three 300 to 400 m bore holes that penetrate the lower part of the FB Formation through to the basal green pelites. They confirm beyond doubt that in the manganese protore, Cu and Ni (Fig. 3e and j) and Co and Cr (see Fig. 3l, and also Tables 2–4) are associated with Mn and Fe (see Fig. 3). On a smaller scale, of course, these elements are not associated with Fe and Mn which are resident for the most part in carbonates (see Fig. 3f and i), whereas Cu and Ni (Co and Cr) are in pyrite. Iron is concentrated in the lower 200 m or so of the FB Formation, whereas Mn is dominant in the upper portion of each bore hole. Presumably this situation arose as a consequence of changing Eh and pH conditions through time in a stagnant portion of an ocean basin. Because the age of the enclosing sediments is coincident with a great period of iron formation development, it is tempting to speculate that perhaps ferrous iron acted as an oxygen acceptor for microorganisms, which in turn served as a source of O_2 for the oxidation of Fe and Mn (cf. Holland, 2002). Since the redox potential required to convert iron from the ferrous to ferric state is far lower than that required to convert $Mn^{2+} \rightarrow Mn^{3+}$, the behavior of the Fe/Mn ratio in the stratigraphic sequence (Fig. 3a–d and h) may mirror events ca. 2 Ga ago, as production of O_2 gradually surpassed the storage capacity of oxygen consuming reservoirs such as Fe^{2+} and Mn^{2+} (and sulfur).

6. Geochemistry of the solid bitumens

Many workers have evaluated the role of solid bitumens in ore genesis (e.g., Goodarzi and Macqueen, 1990; Disnar and Sureau, 1989; Parnell et al., 1993; Mossman and Nagy, 1996). Their geochemistry is of particular importance because it may provide information on matters as diverse as mineral exploration,

Table 1
Whole rock geochemical data on various black shales and Oklo solid bitumens

	Minimum enrichment values, average black shale[a]	U.S.G.S. ref. SDO-1[b]	Alum[c] shale	Mecca[d] shale	AOK average FB Formation black shale[e]	Range, FB Formation black shale[f]	Bitumen #59 FB Formation	Bitumen #35, 50 m from reactor
Ti	7000	7100 r			4900	4600–5400		
Mn	1000	400 r		250	300	200–600		
Ag	7	0.092–0.17 rg	1		2.5	0.04–11.10	n.d.	0.61
Au (ppb)	n.d.	0.002–0.0035 rg			0.0020-0.0075	0.0020–0.0170 0.017		
B	200	128 ave			n.d.	n.d.		
Ba	1000	397 r	500	300	1436	726–2224	0.53	30.8
Co	30	46.8 r	50	400	4.7	2.0–12.9		
Cr	700	66.4 ave	94		189	53–822		
La	70	38.5 r	n.d.		45.3	35.3–56.6	0.15	n.d.
Mo	200	134 r	270	1100	6	2–26	n.d.	1.78
Ni	300	99.5 r	160	400	47	18–105		
Sc	30	13.2 r			8.6	7.2–9.6		
Sr	1500	75.1 r			94	68–116	0.27	12.4
Rb	n.d.	126 ave			139	70–176	0.06	0.58
V	1000	160 r	680	1800	76	50–119	1.97	49.9
Zn	1500	64.1	150	1500	74	10–174		
U	30	48.8	206	130	10.8	2.5–25.7	2.13	185081
Th	n.d.	10.5 r			11.5	8.7–18.4	0.03	0.61
As	n.d.	68.5	17	30	6	1–20		

a, after Vine and Tourtelot (1977); b, recommended values for U.S.G.S. Standard Devonian Oil Shale SDO-1, after Huyck (1990); c and d, after Leventhal (1993); e, average Oklo black shale (AOK), Mossman et al. (1998); f, range of values for FB Formation black shales; g, analysis of solid bitumen in the FB Formation (sample #59); h, solid bitumen 50 m from a fossil nuclear fission reactor (sample #35). Values in ppm; ave, average; r, recommended; rg, range.

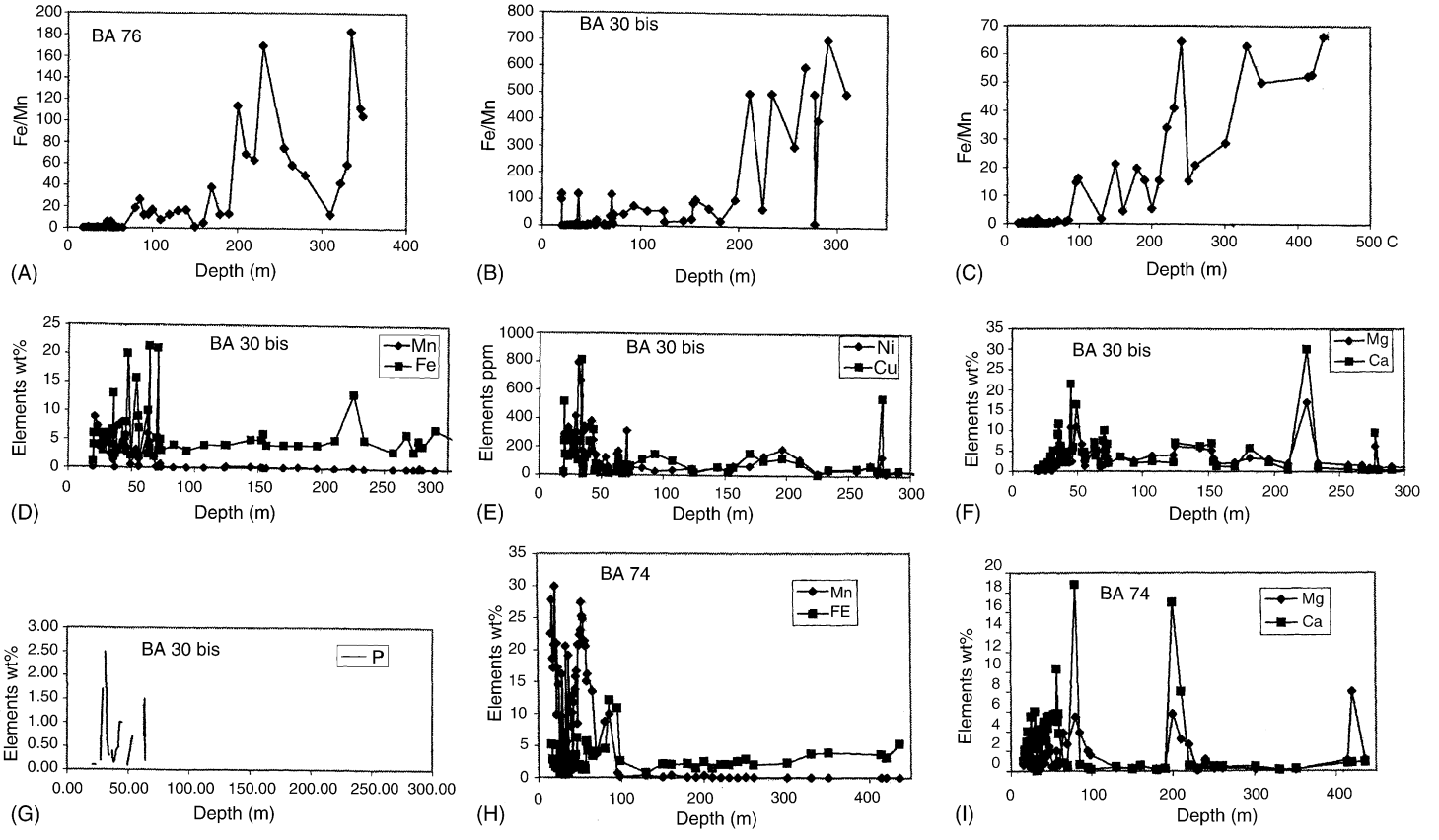

Fig. 3. Geochemical profiles through three (COMILOG) bore holes near the manganese mine at Moanda. Analysis by atomic absorption spectrometry (Azzibrouch-Azziley, 1986). Bore holes penetrate the lower portion of the FB Formation below the manganese ore horizon and through to the green pelites at the base of the formation. All depths are in meters. In all cases zero depth represents the surface of the earth. Profile of Fe/Mn ratios in bore hole (A) BA 76; (B) BA 30 bis; (C) BA 74. Plot of (D) Mn and Fe contents in bore hole BA 30 bis; (E) Ni and Cu contents in bore hole BA 30 bis; (F) Mg and Ca contents in bore hole BA 30 bis; (G) P content in bore hole BA 30 bis; (H) Fe and Mn contents in bore hole BA 74; (I) Mg and Ca contents in bore hole BA 74; (J) Ni and Cu contents in bore hole BA 74; (K) P content in bore hole BA 74; (L) Co, Cr, Pb and Zn in bore hole BA74.

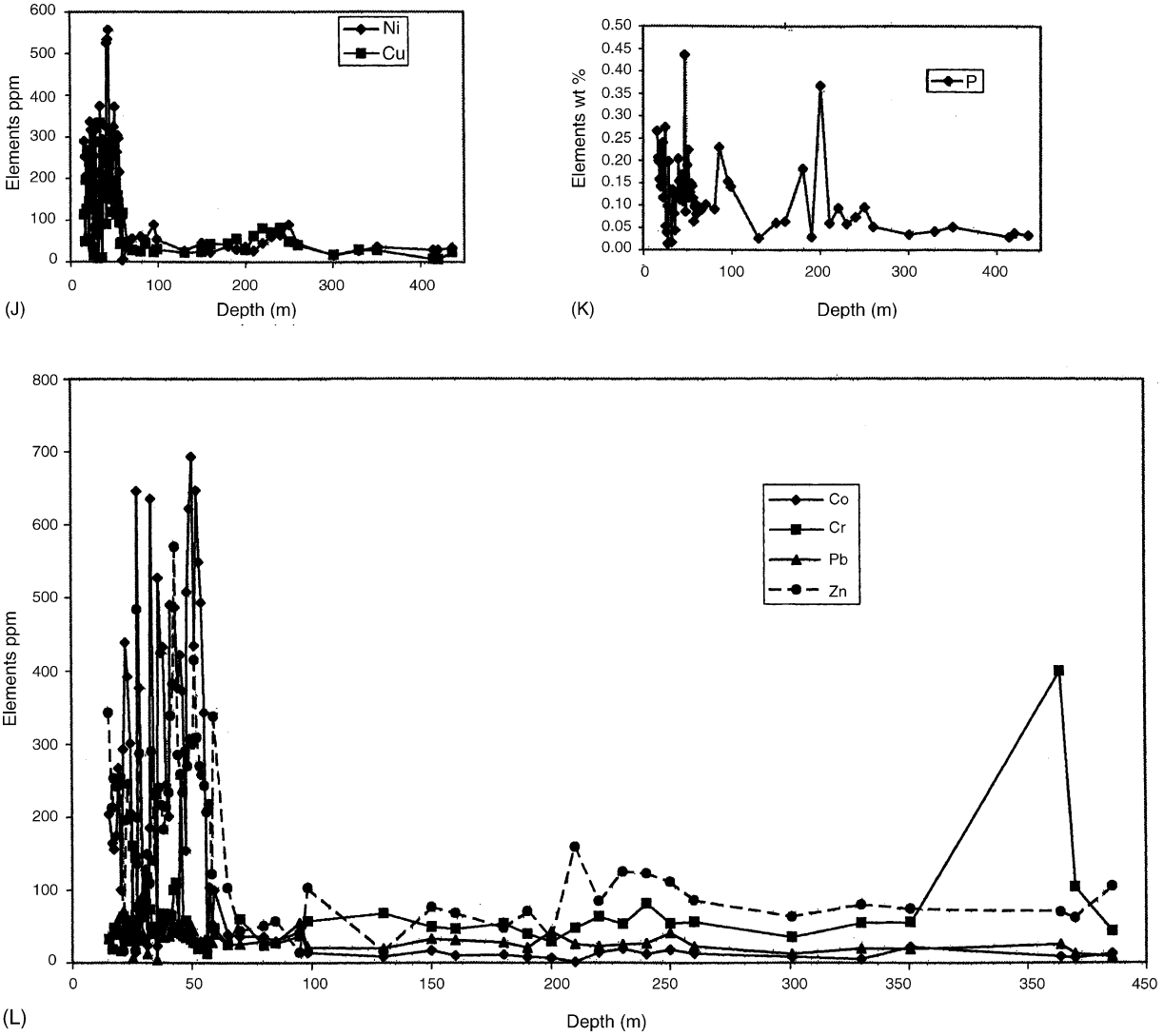

Fig. 3. (*Continued*).

optimum ore recovery procedures, site remediation, etc. (see Parnell et al., 1993).

Mossman and Nagy (1996) and Mossman et al. (2001) have reported on the geochemistry of kerogen and several different types of (solid) bitumens associated with the FB Formation black shales and the uranium ores and fossil nuclear fission reactors of Oklo. These organic materials are distinguished on the basis of field evidence, carbon isotopic signatures, thermal maturation and by geochemical analysis carried out by laser ablation ICP-MS (LA-ICP-MS). This latter technique, as described by Norman et al. (1996), is ideal for providing quantitative in situ trace-element and isotopic analysis of bitumens. For example, using LA-ICP-MS we have found that variations in metal concentrations in Oklo solid bitumens provides an important basis for distinguishing among the several types of bitumens associated with the uranium ores (Jackson and Mossman, 1999). A comparison of analyses #59 and #35 (see Table 1) illustrates the considerable chemical differences among the bitumens.

Table 2
Geochemical data on samples through (COMILOG) bore hole BA76

No.	Depth (m)	Facies	MnO_2 (wt.%)	SiO_2 (wt.%)	Al_2O_3 (wt.%)	FeO (wt.%)	MgO (wt.%)	CaO (wt.%)	K_2O (wt.%)	P_2O_5 (wt.%)	Ni (ppm)	Co (ppm)	Cr (ppm)	Pb (ppm)	Zn (ppm)	Cu (ppm)	Fe/Mn
1	18.4	Amp.	24.1	20.1	5.25	1.6	0.45	3.25	1.7	0.154	399	531	27	33	238	134	0.07
2	19.4	Amp.	25.8	21.6	5.28	1.83	0.38	1.88	1.6	0.144	377	524	26	34	273	135	0.07
3	20.4	Amp.	26.2	20.8	4.5	1.92	0.55	2.7	1.5	0.135	368	521	27	35	261	121	0.07
4	21.4	Amp.	24.9	17.5	4.5	1.65	0.35	3.89	1.5	0.156	287	452	26	36	277	195	0.07
5	22.4	Amp.	21.9	27.2	5.6	2	0.25	2.75	1.8	0.16	321	471	32	38	272	208	0.09
6	23.4	Amp.	20.3	20.8	4.13	2.1	1.15	6.28	1.5	0.105	220	231	26	30	241	79	0.10
7	24.4	Amp.	18.6	20.3	5.4	3.9	0.58	4.41	1.8	0.147	288	350	55	34	180	68	0.21
8	25.4	Amp.	21.6	18.7	4.75	1.23	0.65	5.13	1.6	0.156	341	573	31	41	272	150	0.06
9	26.4	Amp.	22.7	16	4.85	1.2	0.78	5.75	1.6	0.192	364	589	24	38	246	140	0.05
10	27.4	Amp.	25.7	17	4.25	1.68	0.5	4.23	1.4	0.152	336	536	17	29	344	137	0.07
11	28.8	Amp.	24	14.1	4.45	1.68	0.63	5.68	1.5	0.137	304	473	26	37	320	190	0.07
12	29.4	Amp.	24.7	14	4.3	1.5	0.63	5.35	1.5	0.159	332	522	25	39	296	150	0.06
13	30.4	Amp.	23.8	16	4.4	1.35	0.68	5.35	1.5	0.129	255	416	23	33	290	123	0.06
14	31.4	Amp.	24.1	1.1	4.55	1.42	0.73	5.85	1.6	0.134	243	421	23	32	279	154	0.06
15	32.4	Amp.	20	2.1	4.158	1.67	0.68	5.8	1.5	0.14	259	425	2	27	252	151	0.08
16	33.4	Amp.	21.2	17.4	5.17	3.1	0.88	5.75	1.7	0.085	152	148	34	33	297	131	0.15
17	34.4	Amp.	12.4	32	6.6	3.2	0.98	5.73	1.9	0.178	102	58	64	26	106	58	0.26
18	35.4	Amp.	17.6	15	3.6	5	1.63	7	1.2	0.133	204	306	27	26	213	111	0.28
19	36.4	Amp.	20.3	19.6	5.6	1.95	0.73	5.15	1.8	0.141	211	390	36	39	363	159	0.10
20	37.4	Amp.	22.5	16.8	4.5	1.76	0.68	5.7	1.4	0.148	234	421	29	34	321	117	0.08
21	38.4	Amp.	21.2	17.6	5	2.75	0.9	5	1.6	0.075	194	226	33	39	312	136	0.13
22	39.4	Amp.	21.3	18.1	5.6	2.15	0.85	5.2	1.7	0.102	119	152	31	26	320	133	0.10
23	40.4	Amp.	22.5	1.2	1.18	1.92	3.2	9.15	0.8	0.092	82	62	15	20	130	30	0.09
24	41.4	Amp.	15.7	19	4.1	7.1	1.3	5.35	1.4	0.097	54	68	43	20	159	65	0.45
25	42.4	Amp.	9.88	33.2	6.1	7	0.45	4.1	3.1	0.099	58	36	64	23	62	40	0.71
26	43.4	Amp.	16.9	19.3	5.2	6.2	1.18	4	1.7	0.165	67	43	57	19	109	53	0.37
27	44.4	Amp.	5.34	41.8	13	4.15	0.63	3.23	2.5	0.099	114	41	85	27	127	54	0.78
28	45.4	Amp.	3.34	33.8	7.6	3.9	1.9	8.6	1.6	0.157	76	26	69	32	71	38	1.17
29	46.4	Amp.	0.75	41	10.75	4.25	0.98	4.8	2.2	0.145	47	23	104	27	65	43	5.67
30	47.4	Amp.	0.45	56.8	10.7	2.18	0.53	3.03	2.1	0.101	36	19	180	16	47	21	4.84
31	48.4	Amp.	0.7	48.4	8.2	2.82	1.03	5.13	1	0.101	46	18	194	19	25	24	4.03
32	49.4	Amp.	5.98	31.2	11.6	9.5	0.33	2.65	2.1	0.64	112	52	218	22	50	67	1.59
33	50.4	Amp.	5.17	26	3.6	4.35	2.33	9.8	1.2	0.088	40	25	52	21	22	15	0.84
34	51.4	Amp.	2.05	21.7	2.75	11.6	1.5	5.35	1.1	0.26	24	21	62	14	26	12	5.66
35	52.4	Amp.	4.94	44.6	6.9	5.6	0.68	3.5	1.8	0.108	110	63	70	25	72	31	1.13
36	53.4	Amp.	22.02	12.2	1.58	5	1.18	4	1	0.129	205	230	41	14	163	38	0.23
37	54.4	Amp.	23.4	8.5	1.4	3.78	1.45	4.63	1.1	0.094	216	222	3	12	140	36	0.16
38	55.4	Amp.	11.5	24.4	3.85	9.5	1.1	4.35	1.5	0.236	105	97	66	26	68	49	0.83
39	56.4	Amp.	8.5	28.6	3.85	11	0.55	2.5	1.5	0.236	137	253	76	24	114	74	1.29

40	57.4	Amp.	20.1	17.8	4.1	5.1	0.7	4.83	1.5	0.067	199	484	35	28	263	174	0.25
41	58.4	Amp.	12.6	28.6	8.8	6.6	0.4	3	2.4	0.162	102	208	59	29	200	176	0.52
42	59.4	Amp.	13.6	28.5	8.3	4.4	0.4	4.15	2.3	0.22	123	139	55	46	163	173	0.32
43	60	Amp.	12.3	31	8.6	4.6	0.18	0.51	1.6	0.164	103	112	31	60	165	147	0.37
44	65	Dol.	1.7	7.5	2.63	0.65	9.25	23.8	0.43	0.087	12	9	18	31	19	7	0.38
45	80	GRES	0.12	74	8.52	2.25	0.23	0.21	1.26	0.066	50	10	39	20	97	63	18.75
46	85	Amp.	0.11	66.1	12.8	2.95	0.32	0.25	1.9	0.059	30	10	44	21	89	45	26.82
47	90	Amp.	0.17	63.7	13.3	2.06	0.25	0.36	1.7	0.044	46	11	58	28	93	80	12.12
48	95	Amp.	0.18	63.7	14.1	2.26	0.31	0.31	2	0.051	45	17	53	20	109	74	12.56
49	100	Amp.	0.12	66.4	12.1	2.06	2.6	1.9	2.2	0.053	46	10	39	33	85	52	17.17
50	110	Amp.	0.18	6	10.9	1.37	3	2.5	2.08	0.074	41	8	42	40	85	60	7.61
51	120	Amp.	0.19	65.8	10.9	2.39	3.5	2.33	1.76	0.068	38	8	39	39	108	57	12.58
52	130	Amp.	0.13	65	12.2	2.1	3.65	2	1.8	0.061	31	6	39	36	80	41	16.15
53	140	P.R.	0.15	63.2	14	2.57	3.65	1.6	2.04	0.117	41	7	45	31	85	47	17.13
54	150	Amp.	5.4	40.4	5.65	8	5.75	3.68	0.71	0.115	68	96	29	66	316	44	1.48
55	160	P.R.	0.46	52.9	8.7	2.3	6.68	5.2	0.8	0.071	36	13	29	45	68	70	5.00
56	170	P.R.	0.07	67.6	13.6	2.66	2.11	1.1	1.84	0.098	44	8	54	34	157	18	38.00
57	180	Amp.	0.18	57.4	1	2.28	4.3	3	2.44	0.031	44	5	55	38	72	33	12.67
58	190	Amp.	0.23	61.8	19	3.05	1.8	0.85	2.56	0.082	32	11	50	35	65	29	13.26
59	200	Amp.	0.17	51.7	12.8	19.3	4.3	4.3	2.24	0.104	88	10	43	30	113	59	113.53
60	210	Amp.	0.05	56	22.6	3.46	1.83	2.2	2.8	0.039	69	8	60	33	100	4	69.20
61	220	Amp.	0.02	55.3	16.9	1.27	0.78	0.63	2	0.055	58	6	59	32	108	66	63.50
62	230	Amp.	0.02	52	25	3.39	0.7	0.38	2.88	0.032	90	18	59	40	156	74	169.50
63	255	Amp.	0.04	58.8	21.3	3	1.58	1.38	2.68	0.038	25	6	51	34	85	31	75.00
64	265	Amp.	0.05	62	20.3	2.95	1.35	1.2	3	0.035	41	17	48	26	70	25	59.00
65	280	GRES	0.03	73.8	16.6	1.49	0.7	0.33	3.4	0.02	26	3	90	24	37	27	49.67
66	310	GRES	0.09	91.6	3.96	1.17	0.53	0.6	0.76	0.005	6	1	8	24	21	3	13.00
67	322	AMP	0.07	65.1	23	2.95	0.58	0.33	3.48	0.039	47	12	64	25	100	15	42.14
68	330	P.V.	0.04	62.7	25.1	2.38	0.75	0.35	4.16	0.031	40	10	67	15	67	16	59.50
69	334	P.V.	0.02	60	24.8	3.66	0.55	0.33	4.84	0.029	35	11	209	19	73	3	183.00
70	345	P.V.	0.03	61	23	3.36	0.45	0.58	4.6	0.022	32	11	30	15	75	13	112.00
71	348	P.V.	0.04	60	22.7	4.2	0.58	0.68	4.6	0.027	35	12	47	16	77	23	105.00

Elements Mn through P in wt.% oxides; elements Ni through Cu in ppm. Amp.: black shale; P.R.: pelite rubanée (ribbon shale); GRES.: quartzose arenite; P.V.: pelite verte (green shale).

Table 3
Geochemical data on samples through (COMILOG) bore hole BA 30 bis

No.	Depth (m)	Facies	MnO (wt.%)	SiO_2 (wt.%)	Al_2O_3 (wt.%)	FeO (wt.%)	MgO (wt.%)	CaO (wt.%)	K_2O (wt.%)	P_2O_5 (wt.%)	Ni (ppm)	Co (ppm)	Cr (ppm)	Pb (ppm)	Zn (ppm)	Cu (ppm)	Fe/Mn
1	19.35	Sand.	0.01	87.0	6.0	1	0.1	0.4	1.2		29	13	30	17	32	17	100
2	19.75	Amp.	0.05	76.0	30.0	6	0.6	0.3	3.6		5	128	144	101	98	518	120
3	20	Amp.	6.07	40.0	10.0	4	0.1	0.7	2.1		293	517	19	61	235	242	1
4	20.55	Amp.	8.88	23.4	6.3	4	0.63	0.5	1.1	0.1	274	495	136	999	291	142	0
5	23.2	Amp.	7.32	25.6	6.9	4	1.72	1.5	1.33	0.1	335	553	90	999	335	128	1
6	25.15	Amp.	3.51	65.0	13.0	6	0.1	1.3	2		303	374	50	54	168	243	2
7	27.15	Amp.	4.92	38.5	9.3	3	1.82	2.1	1.69	0.2	268	299	75	999	210	185	1
8	29	Amp.	4.17	29.3	8.3	5	1.09	3.6	1.52	1.7	417	528	63	999	406	139	1
9	30.05	Amp.	5.30	65.0	13.0	6	0.1	1.3	2		303	374	50	5.4	168	243	1
10	31.15	Amp.	4.85	27.6	6.0	5.3	1.93	5.1	1.11	2.5	794	570	92	999	663	106	1
11	32.8	Amp.	2.54	41.0	11.7	6.1	1.4	2.2	2.23	0.6	670	512	94	999	224	237	2
12	34	Amp.	2.52	39.7	12.2	5.7	1.35	1.6	2.38	0.3	297	300	69	999	200	813	2
13	34.9	Amp.	1.65	37.6	6.7	6.6	5.94	9.2	1.15	0.3	174	63	40	999	138	79	4
14	35.2	Amp.	1.51	58.0	6.0	2	4.9	8.9	0.8			29	2.47	17	75	6	1
15	35.45	Amp.	1.35	35.0	6.0	13	6.1	11.7	1.5		120	37	56	49	113	66	10
16	35.8	Amp.	1.70	52.0	9.0	4	6.9	11.6	1.5		309	79	70	23	606	53	2
17	36.8	Amp.	0.02	15.9	3.9	2.4	2.62	6.3	0.157	0.4	345	723	104	999	267	119	120
18	38.4	Amp.	7.32	19.7	5.4	3.4	2.22	4.1	0.915	0.15	332	647	51	999	407	144	0
19	40.35	Amp.	7.44	18.4	5.4	3.3	2.16	4.1	0.98	0.4	346	1094	98	999	490	239	0
20	41.85	Amp.	7.90	14.9	4.4	3	2.25	4.8	0.81	0.5	380	629	96	999	457	163	0
21	43.15	Amp.	4.80	31.3	3.6	3.8	2.15	3.4	1.63	1	247	400	72	999	394	320	1
22	44.65	Amp.	2.88	7.3	2.1	5.5	10.9	21.4	0.34	1	152	515	33	999	185	31	2
23	45.5	Amp.	5.89	35.0	7.0	8	2.4	5	1.6		140	89	36	33	426	74	1
24	46.5	Amp.	3.55	23.0	5.0	20	6.1	5.9	1.2		64	32	67	47	91	61	6
25	49.2	Amp.	0.57	29.1	6.1	2.2	11	16.4	1	0.1	70	22	38	999	116	13	4
26	53.2	Amp.	3.26	25.6	7.9	15.8	6.68	4.7	0.45	0.7	125	38	76	999	110	25	5
27	55.1	Amp.	1.70	52.0	11.0	9	2.4	4.8	2.1		57	43	117	31	75	33	5
28	55.6	Sand.	0.35	93.0	3.0	7	1.3	3	1.3		37	23	546	32	54	24	20
29	55.7	Sand.	0.23	31.0	6.0	2	1.3	4	0.6		14	10	413	17	53	7	9
30	62.6	Amp.	6.07	35.0	4.0	10	5.8	5.6	0.6		26.4	267	66	12	213	46	2
31	62.8	Amp.	2.73	46.0	3.8	2.4	4.92	7.2	0.47	0.7	150	50	23	999	152	18	1
32	63.5	Amp.	3.60	17.4	2.7	21.3	4.68	3.8	0.4	1.5	140	120	39	999	151	51	6
33	63.95	Amp.	4.60	21.1	4.8	3.4	5.12	5.1	95	0.2	171	312	83	999	222	104	1
34	67.45	Sand.	1.92	91.0	8.0	2	1	2.2	1.2		17	10	482	16	56	7	1
35	69.4	Amp.	0.15	34.0	6.7	5.2	5.12	7.6	1.79	0.4	73	35	63	999	117	26	35
36	70.4	Amp.	0.18	49.0	9.0	21	1.6	10	1.8		314	163	1268	188	143	70	117
37	71.1	Sand.	0.11	83.0	12.0	3	2.3	4.1	1.5		28	10	130	12	29	24	27
38	71.5	Sand.	0.30	75.0	14.0	4	4.9	5.8	1.9		48	10	171	21	103	38	13
39	72.4	Sand.	0.66	78.0	7.0	5	3.5	6.8	0.7	0.7	10	10	423	20	10	20	8

40	73.4	Sand.	0.07	79.0	17.0	3	1.9	2	3.1	53	11	162	26	90	62	43
41	83	Sand.	0.09	15.0	15.0	4	3.6	3.5	2.6	52	10	16.4	23	66	111	44
42	93.35	Amp.	0.04	67.0	21.0	3	2.7	2.1	2.1	28	10	149	12	153	148	75
43	107.3	Sand.	0.07	81.0	14.0	4	3.9	2.5	2	37	10	117	18	88	102	57
44	123.5	Sand.	0.07	53.0	12.0	4	4	2.2	1.9	47	10	140	25	92	39	57
45	124.65	Amp.	0.24	68.0	11.0	4	6.2	7.1	1.6	26	10	97	17	69	20	17
46	144	Sand.	0.24	78.0	14.0	5	5.8	6.2	1.6	59	10	250	23	93	57	21
47	152.5	Amp.	0.19	60.0	15.0	5	5.3	7	2.2	25	10	123	15	56	21	26
48	154	Amp.	0.07	64.0	20.0	6	3.3	2.4	3	34	10	119	38	90	51	86
49	156.4	Sand.	0.04	76.0	19.0	4	1.9	1.3	3	66	10	148	28	191	56	100
50	170	Sand.	0.06	74.0	21.0	4	2.3	1.2	3.1	65	10	188	16	153	157	67
51	181.4	P.R.	0.21	70.0	20.0	4	3.3	5.7	2.4	139	10	190	23	177	102	19
52	196.3	P.R.	0.04	70.0	22.0	4	3.1	2.3	2.4	186	14	169	35	111	121	100
53	210.6	Amp.	0.01	67.0	28.0	5	2	0.5	2.2	115	13	139	42	157	89	500
54	225	DOL.	0.20	8.0	4.0	13	17	30	0.6	16	10	30	14	10	5	65
55	233.75	Amp.	0.01	71.0	28.0	5	2.2	1	2.4	35	10	123	22	67	43	500
56	256.75	Sand.	0.01	75.0	28.0	3	1.7	0.7	2.6	37	10	144	17	45	46	300
57	267.35	P.R.	0.01	74.0	25.0	6	1.6	0.5	2.8	71	23	159	51	76	66	600
58	273.1	P.R.	0	57.0	30.0	3	1	0.4	3	16	10	123	21	60	38	
59	276.7	P.R.	0.01	63.0	25.0	5	0.7	0.5	3.2	131	76	188	148	67	545	500
60	277.5	P.R.	0.30	79.0	4.0	4	6.3	9.6	0.8	26	13	382	26	24	27	13
61	280.15	Sand.	0.01	66.0	26.0	4	0.9	0.4	3.8	15	10	255	11	20	30	400
62	290.2	P.V.	0.01	68.0	23.0	7	1.2	0.4	3.4	36	10	138	126	73	36	700
63	309.2	P.V.	0.01	66.0	24.0	5	0.9	0.4	5	23	10	98	18	60	15	500

Concentrations, abbreviations, analytical procedure as for Table 2. Amp.: black shale; P.R.: pelite rubanée (ribbon shale); Sand.: sandstone; DOL.: dolomite; P.V.: pelite verte (green shale).

Table 4
Geochemical data on samples through (COMILOG) bore hole BA 74

No.	Depth (m)	Facies	MnO_2 (wt.%)	SiO_2 (wt.%)	Al_2O_3 (wt.%)	FeO (wt.%)	MgO (wt.%)	CaO (wt.%)	K_2O (wt.%)	P_2O_5 (wt.%)	Ni (ppm)	Co (ppm)	Cr (ppm)	Pb (ppm)	Zn (ppm)	Cu (ppm)	Fe/Mn
1	15.4	Amp.	22.6	23.0	3.9	5.2	0.63	0.98	1.1	0.266	289	204	32	35	343	113	0.23
2	16.75	Amp.	27.8	18.0	2.76	2.8	0.98	2.1	0.8	0.208	253	164	18	19	213	48	0.10
3	17.4	Amp.	18.6	30.5	6.58	2.73	1.35	1.48	1.9	0.198	204	156	48	45	253	196	0.15
4	18.4	Amp.	17.2	31.7	6.35	2.14	0.88	0.88	1.9	0.158	248	174	45	45	242	126	0.12
5	19.4	Amp.	20.8	21.2	7	2.4	1.7	2.9	1.5	0.142	269	267	38	61	243	268	0.12
6	20.4	Amp.	29.9	10.1	2.14	1.7	1.73	4	0.7	0.222	203	100	16	18	255	54	0.06
7	21.4	Amp.	9.9	39.7	8.15	5.05	0.85	2	1.9	0.24	211	293	63	71	16	145	0.51
8	22.4	Amp.	21.0	21.7	5.72	1.46	1.5	4	1.3	0.117	336	439	29	40	196	172	0.07
9	23.4	Amp.	17.2	28.1	7.1	1.93	1.33	3	1.8	0.192	317	392	42	48	245	231	0.11
10	24.4	Amp.	14.6	32.5	6.87	2.25	0.33	5.5	1.9	0.274	314	301	50	57	204	190	0.15
11	25.4	GRES	2.66	76.6	6.7	0.83	0.4	1.13	1.3	0.053	83	52	160	6	59	35	0.31
12	26.4	GRES	2.92	67.2	5.5	0.78	1.1	2.25	1.1	0.04	31	14	144	19	17	15	0.27
13	27.2	Amp.	9.7	41.0	14.3	2.8	1.25	2.25		0.098	255	135	76	35	199	184	0.29
14	27.4	Amp.	9.65	41.5	12.7	2.96	1.18	3.91	0.9	0.013	332	646	30	42	484	213	0.31
15	28.4	Amp.	16.2	25.8	5.4	4.1	1	3.3	1.7	0.198	316	377	64	86	287	287	0.25
16	29.4	Amp.	5.47	51.2	7.6	2.4	1.15	6	1.3	0.093	104	76	67	39	62	65	0.44
17	30.4	Amp.	7.08	36.5	4.98	4.4	1.1	2.83	2.1	0.093	138	128	81	31	93	113	0.62
18	31.4	Amp.	2.62	60.0	3.45	0.5	1.2	7.00	0.4	0.017	63	24	116	12	149	8	0.19
19	32.4	Amp.	5.93	41.4	7.85	5.6	0.53	3.7	2	0.135	186	185	73	40	109	92	0.94
20	33.4	Amp.	20.59	21.0	5.75	1.92	1.2	4.2	1.4	0.125	374	635	43	41	290	333	0.09
21	34.4	Amp.	5.56	46.0	1.8	3.12	0.8	2.23	1.6	0.081	210	231	49	46	140	180	0.56
22	35.4	Amp.	1.27	30.4	5.85	0.75	0.18	0.55	1.2	0.044	88	23		4	234	9	0.59
23	36.4	Amp.	19.1	24.6	6.2	1.85	1	3.5	1.6	0.12	294	527	49	43	240	172	0.10
24	37.4	Amp.	12.6	33.3	8.4	2.3	0.85	3.13	2	0.125	239	425	61	48	216	200	0.18
25	38.4	Amp.	12.4	35.6	7.27	2	1	3.58	2.7	0.124	250	433	67	35	183	152	0.16
26	39.4	Amp.	8.04	36.6	10	3.48	1	3.75	2.1	0.204	237	244	60	60	214	272	0.43
27	40.4	Amp.	10.22	39.0	7.05	1.8	1.3	4.95	1.6	0.153	324	201	66	37	234	90	0.18
28	41.4	Amp.	1.31	30.1	8.6	2.42	0.8	3.3	2	0.112	525	490	64	58	339	249	1.85
29	42.4	Amp.	11.79	32.5	8.45	2.95	1.75	3.43	1.8	0.115	535	488	100	47	382	181	0.25
30	43.4	Amp.	13.15	27.8	10.28	3.47	1.53	3	2.5	0.169	557	487	110	42	570	286	0.26
31	44.4	Amp.	13.83	7.0	8.5	3.5	1.5	5.4	1.5	0.109	224	377	48	55	285	256	0.25
32	45.4	Amp.	15.81	29.2	6.6	1.7	1.88	4.3	1.5	0.163	255	422	39	259	259	173	0.11
33	46.4	Amp.	16.7	19.9	4	6.2	1.78	5.4	1	0.436	308	373	37	40	234	119	0.37
34	47.4	Amp.	8.5	40.9	8.1	1.92	2.45	5.53	1.8	0.086	184	154	58	35	290	150	0.23
35	48.4	Amp.	20.8	20.9	5.1	1.95	1.95	5.13	1.3	0.146	270	508	36	47	270	153	0.09
36	49.4	Amp.	20.7	19.5	5.3	1.95	1.95	5.4	1.3	0.19	324	622	32	52	307	168	0.09
37	50.4	Amp.	22.4	17.6	4.6	1.58	0.43	5.1	1.2	0.224	372	693	28	44	300	165	0.07
38	51.4	Amp.	23.1	14.9	4.21	1.78	0.48	5.48	1.1	0.117	197	435	27	28	415	180	0.08
39	52.4	Amp.	27.4	11.3	2.38	1.3	0.48	5.7	0.9	0.13	264	647	19	26	309	113	0.05

40	53.4	Amp.	25.3	12.0	3.75	1.56	0.38	5.2	1	0.149	304	549	24	30	270	158	0.06
41	54.4	Amp.	24.8	13.6	4	1.78	0.4	5.4	1.1	0.143	296	493	27	25	258	140	0.07
42	55.4	Amp.	21.5	16.0	3.84	1.75	0.73	5.73	1.1	0.116	216	343	28	32	243	94	0.08
43	56.4	DOL.	21.4	6.80	1.15	1.2	2	10.3	0.5	0.064	105	16	12	23	207	43	0.06
44	57.4	Amp.	20.6	14.5	3.47	5.6	0.63	5	0.9	0.096	89	104	30	28	218	112	0.27
45	58.4	Amp.	15.1	21.1	4.2	5.7	0.98	5.8	0.8	0.103	4	53	48	28	122	46	0.38
46	59.4	Amp.	16.2	22.8	6.45	4.2	0.6	3.8	1.1	0.08	6	100	48	40	338	117	0.26
46b	65	Amp.	13.5	21.6	5.14	3.37	3.85	0.8	0.85	0.09	45	39	25	25	103	36	0.25
47	70	Amp.	3.66	48.0	8.83	4.04	2.74	0.5	1.5	0.102	56	36	60	26	44	28	1.10
48	80.1	DOL.	8.76	11.4	1.95	4.47	5.5	18.8	0.34	0.091	61	36	24	30	51	25	0.51
49	85	Amp.	9.95	18.9	4.02	12.1	3.9	0.65	0.68	0.23	54	30	27	28	57	43	1.22
50	95.1	Amp.	0.75	53.0	5.04	10.9	2.06	0.31	0.89	0.153	90	43	37	55	14	24	14.53
51	98.5	GRES	0.16	63.0	16.3	2.57	1.6	0.17	2.55	0.142	54	14	57	21	103	30	16.06
52	129.9	GRES	0.45	74.0	3.95	0.81	0.3	0.4	0.24	0.027	27	9	68	20	16	22	1.80
53	150	Amp.	0.1	67.6	12.8	2.12	0.28	0.18	1.9	0.061	46	17	49	33	76	25	21.20
54	160	Amp.	0.46	58.6	7.35	2.08	0.53	0.55	0.74	0.064	23	10	46	31	68	43	4.52
55	180	P.R.	0.11	70.3	13.9	2.18	0.21	0.12	2.3	0.182	38	11	54	28	48	44	19.82
56	190.1	P.R.	0.1	72.4	7.7	1.55	0.3	0.22	1.22	0.03	31	8	40	21	71	55	15.50
57	200	DOL.	0.45	38.0	4.8	2.5	5.75	17	0.38	0.368	37	7	29	43	35	29	5.56
58	210	P.R.	0.1	61.0	8.35	1.54	3.25	8	0.9	0.06	28	1	48	26	159	62	15.40
59	220	P.R.	0.06	58.4	16.1	2.05	2.7	0.55	1.95	0.094	46	14	63	23	85	81	34.17
60	230	Amp.	0.05	60.0	17.4	2.05	0.13	0.26	2.7	0.059	61	19	53	25	125	71	41.00
61	240	Amp.	0.04	53.0	24	2.58	1.2	0.58	2.4	0.074	65	12	81	27	123	82	64.50
61b	250	Amp.	0.19	51.5	16.1	2.91	0.3	0.49	1.6	0.096	90	18	54	41	111	49	15.32
62	260	Amp.	0.1	53.1	16	2.09	0.33	0.49	1.7	0.052	44	13	56	23	86	41	20.90
63	300.75	Amp.	0.08	62.6	15	2.3	0.2	0.44	1.34	0.035	16	8	35	12	63	17	28.75
64	329.75	Amp.	0.06	56.5	23	3.77	0.13	0.12	1.49	0.042	28	5	55	20	80	30	62.83
65	350.5	Amp.	0.08	56.5	21.7	4	0.16	0.18	1.41	0.051	37	22	56	19	75	29	50.00
66	414	P.V.	0.07	56.7	27.4	3.66	1.1	0.81	3.5	0.03	30	9	400	26	70	7	52.29
67	420	P.V.	0.06	55.0	27.2	3.18	8	0.85	4	0.038	30	7	104	13	62	6	53.00
68	435.75	P.V.	0.08	54.3	27.7	5.3	1.2	0.9	4	0.033	35	13	44	9	105	23	66.25

Concentrations, abbreviations, and analytical procedure as for Tables 2 and 3.

Solid bitumens in the FB Formation and in the uranium ores in the underlying FA Formation contain highly condensed aromatic hydrocarbons and are highly overmature, with H/C and O/C ratios typically 0.5% and 0.3% or less, respectively (Nagy et al., 1991, 1993). LA-ICP-MS analysis of the solid bitumen in the FB Formation reveals that trace-element concentrations are characteristically very low compared with that of the black shales and with the bitumens in the uranium ore (e.g., compare bitumen samples #59 and #35, Table 1). This fact makes it virtually impossible to determine the extent to which the metal content of the FB Formation bitumen may have been derived from the black shale. This is nevertheless an important question, especially in view of current studies of the Oklo analogue to anthropogenic nuclear waste containment (e.g., Curtis et al., 1989; Ewing, 2000; Jancezek, 2000).

The nature of metal concentrations in solid bitumens associated with the uranium ore in and near the fossil, nuclear fission reactor zones, has been singled out for special attention (e.g., Mossman et al., 2000). The work was initiated by the late Professor B. Nagy, and although beyond the scope of this paper to elaborate upon in detail here, a brief status update seems appropriate. Nagy et al. (1991, 1993) showed that organic matter, where present in fossil nuclear fission reactor zones of Oklo, efficiently constrained mobilization and redistribution of uranium and a number of fissiogenic nuclides. Jackson and Mossman (1999) employed LA-ICP-MS to test Oklo solid bitumen samples for large shifts in isotopic ratios attributable to the presence of fissiogenic isotopes. This work focused on bitumens that had been generated by hydrous pyrolysis during criticality. Tests on samples such as bitumen #35 ca. 50 m distant from the Okelobondo reactor yielded no evidence of significant shifts in isotopic ratios. However, one sample (D75-11-1991-22) obtained from a bitumen nodule inside reactor #16 yields clear evidence that, in some instances, fluid bitumen generated by hydrous pyrolysis during criticality may have promoted at least local migration of some fission products. Thus, as shown in Fig. 4, LA-ICP-MS analysis of solid bitumen in reactor #16 yields strong signals for Ru and Rh. There are also clear indications (85–105 AMU) of the fissiogenic origin of REE, the migration of which (at least in the immediate vicinity of the reactor) was presumably promoted by the reducing environment provided by once liquid bitumen. Fig. 5 unmistakably shows several very disturbed ratios, those for Pd, Te,

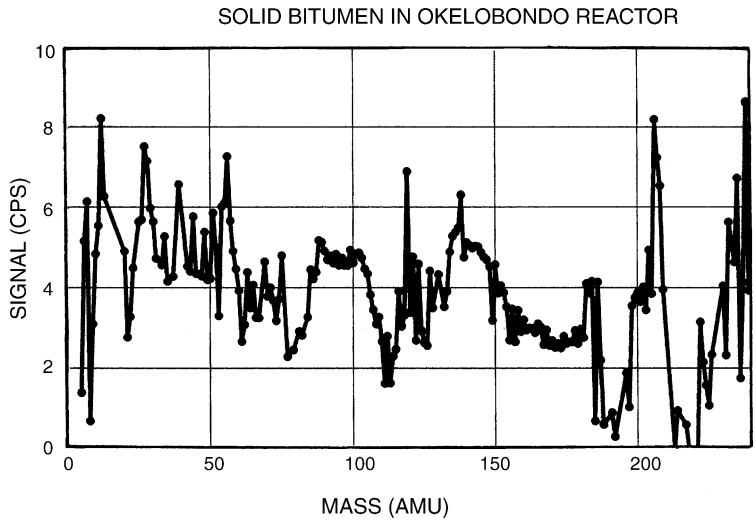

Fig. 4. LA-ICP-MS mass spectral analysis of pitchblende-bearing bitumen; sample D75-11-1991-22 from the Okelobondo reactor. The signals [representing relative concentrations in counts/second (cps)] vs. mass (AMU) plot shows large signals for rare elements (e.g., Ru and Rh), and anomalous isotopic ratios (see Fig. 5) in the regions 85–105 and 140–150 AMU indicate a fissiogenic origin for these enrichments (see text for details).

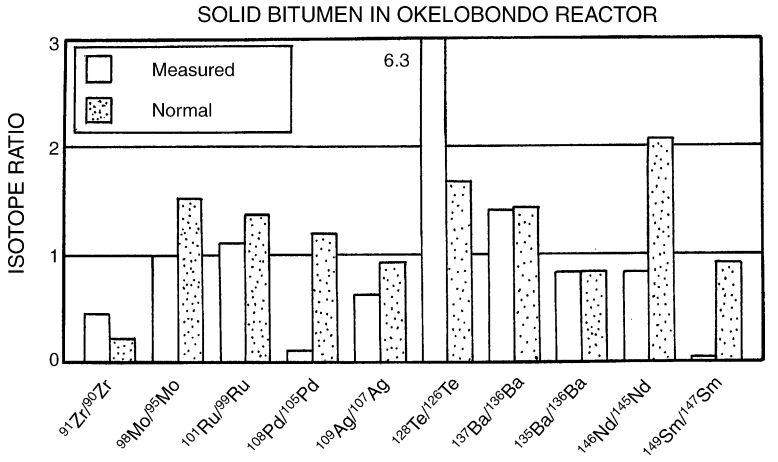

Fig. 5. The isotope ratio plot shows isotopic ratios for selected ratios for certain elements in sample D75-11-1991-22 from the Okelobondo reactor, compared with 'normal' values. For elements except Ba, differences between measured and normal values are statistically significant at the 2 sigma confidence level.

Nd and Sm being radically different from "normal" isotopic ratios (i.e., natural, non-fissiogenic ratios). In fact, they closely mirror the ratios reported by Hidaka and Holliger (1998) for these elements near the cores of reactor zones 10, 13, and the Bangombé reactor. Differences in isotopic ratios between sample and calibration standards present significant problems in terms of performing quantitative analyses of elements with disturbed ratios. Unfortunately, chemical separation of each element from the sample solution (as done by Hidaka and Holliger, ibid) is not an option with laser sampling.

The question arises as to what extent, and over what distance, migration of these metals occurred? Results of LA-ICP-MS analysis indicate that the metals are, in some cases, hosted in carbon, having presumably originated as organometallic complexes; in other cases, they are hosted by aluminous phases (Jackson and Mossman, 1999) the origin of which is unknown. Work is in progress to elucidate the geochemistry of these solid bitumens, with special focus on the Bangombé reactor, the last natural nuclear fission reactor (Blanc et al., 1997). Lying buried only 12 m in a deeply weathered tropical soil, Bangombé serves as an analogue to a worst case scenario of a radioactive waste repository accident. It could be that here, bitumen geochemistry can provide crucial evidence applicable in a predictive sense to the problem of safe containment of nuclear waste.

7. Conclusions

Evolution of the Paleoproterozoic FB Formation black shales is linked to the genesis of the manganese and uranium ores of the Franceville Series. Although the former were concentrated to ore grade by surficial (lateritic) processes during fairly recent geologic history, organic matter played significant roles during initial sedimentation, as well as in what could be termed "ground preparation" during early diagenesis. The organic matter, as various microbial forms of life preserved as fossils in the FB Formation and associated rocks, also served to source prolific amounts of liquid hydrocarbons. The hydrocarbons, reacting in turn with uranium-bearing aqueous solutions led to the formation of the rich uranium ores of Oklo and, subsequently, to the origin of 15 natural nuclear fission reactors. Thus, overall there seems to have been a series of interconnected geological events. The available evidence from the literature and the new analytical data presented in this paper lead us to conclude the following:

(1) The FB Formation provides a good example of metal-lean black shales despite its extraordinarily high organic matter productivity and the excellent degree of organic matter preservation.
(2) In addition to abundant microfossils in the FB Formation, organic matter in the FB and underlying FA formations takes the form of kerogen and several

types of solid bitumen. The kerogen and solid bitumen are highly overmature, with H/C and O/C ratios typically 0.5–0.3% or less, respectively.

(3) Initial maturation of kerogen through the "oil window" led to the production of liquid hydrocarbons equivalent in amount to that of any modern supergiant oil field.

(4) The black shales are enriched only slightly in Cr, Au, Ag, and Ba compared to the standard metalliferous black shale SDO-1. Their trace-element geochemistry most closely resembles that of greywacke shale turbidites of Archean greenstone belts.

(5) LA-ICP-MS in situ analysis of solid bitumens in the FB Formation reveals very low trace-element contents.

(6) Geochemical profiles through the lower part of the FB Formation, below the manganese ore horizon, reveal upward decreasing Fe/Mn ratios compatible with the concept of increased oxidation potential linked to prolific microbial activity.

(7) Analysis of solid bitumen associated with the fossil nuclear reactors of Oklo in the FA Formation reveals that some bitumens, particularly those samples close to reactor cores, are highly enriched in metals hosted in the carbonaceous matrix or in aluminous phases within the matrix.

(8) Among the metals detected in bitumens from reactor zones are highly anomalous amounts of Ru and Rh, and REE that originated as fission products. Indications are that once liquid bitumens, although effective in containing these elements, may nevertheless have led to the migration of fission products beyond the immediate reactor zones. Research continues to examine this possibility and the extent to which bitumens are capable of transporting metals.

Acknowledgements

Dr. F. Weber is thanked for helpful discussions and for providing photomicrographs of Paleoproterozoic microfossils (Fig. 2). We gratefully acknowledge invaluable advice contributed by Ray Coveney and journal referee David Livitz. Analytical support was kindly supplied by the Société Nationale Elf-Aquitaine at Pau (SNEA-P), France, in J. Connan's laboratory. This research is part of the International Geological Correlation Program project 429 (Organics in major environmental issues). It is supported by operating grant A8295 to DJM from the Natural Sciences and Engineering Research Council of Canada.

References

Alpern, B., 1978. Etude pétrographique de la matière organique d'Oklo in Natural Fission Reactors. IAEA, Vienna, pp. 333–351.

Amard, B., Bertrand-Sarfati, J., 1997. Microfossils in 2000 Ga old cherty stromatolites of the Franceville Group, Gabon. Precambrian Res. 81, 197–221.

Arthur, M.A., Sageman, B.B., 1994. Marine black shales: depositional mechanisms and environments of ancient deposits. Annu. Rev. Earth Planet. Sci. 22, 499–551.

Azzibrouch-Azziley, G., 1986. Sédimentologie et géochimie du Francevillien B (Protérozoïque inférieur). Métallogénie des gisements de manganèse du Moanda, Gabon. Thèse Université Louis Pasteur, Strasbourg, 210 pp.

Bertrand-Sarfati, J., Potin, B., 1994. Microfossiliferous cherty stromatolites in the 2000 Ma Franceville Group, Gabon. Precambrian Res. 65, 341–356.

Blanc, P.L., Bruno, J., Gauthier-Lafaye, F., Griffault, L., Ledoux, E., Louvat, D., Michaud, V., Montoto, M., Oversby, V., Perez del Villarr, L., Smellie, J., 1997. The last natural nuclear fission reactor. Nature 387, 337.

Brocks, J.J., Logan, G.A., Buick, R., Summons, R.E., 1999. Archean molecular fossils and the early rise of eukaryotes. Science 285, 1033–1036.

Buick, R., Rasmussen, B., Krapez, B., 1998. Archean oil: evidence for extensive hydrocarbon generation and migration 2.5–3.5 Ga. Bull. Am. Assoc. Pet. Geol. 82 (1), 50–69.

Cortial, F., 1985. Les bitumes du Francevillian (Protérozoïque inferieur du Gabon 2000 Ma) et leurs kérogènes. Relations avec les minéralisations uranifères. Thèse Doct. Université Strasbourg, 217 pp.

Cortial, F., Gauthier-Lafaye, F., Lacrampe-Couloume, G., Oberlin, A., Weber, F., 1990. Characterization of organic matter associated with uranium deposits in the Francevillian Formation of Gabon (Lower Proterozoic). Org. Geochem. 15, 73–85.

Curtis, D., Benjamin, T., Gancarz, A., Loss, R., Rosman, K., DeLaeter, J., Delmore, J.E., Maeck, W.J., 1989. Fission product retention in the Oklo natural fission reactors. Appl. Geochem. 4, 49–62.

de Duve, C., 1996. The birth of complex cells. Sci. Am. 274 (4), 56–63.

Desborough, G., Pittmen, J., Huffman, C., 1976. Concentration and mineral residence of elements in Green River Formation, Colorado and Utah. Chem. Geol. 17, 13–26.

Disnar, J.R., Sureau, J.F., 1989. Organic matter in ore genesis: progress and perspectives. Org. Geochem. 16, 577–599.

Ewing, R.C., 2000. Radioactivity and the 20th century. In: Burns, P.C., Finch, R.J. (Eds.), Uranium: Mineralogy, Geochemistry and

the Environment. Reviews in Mineralogy, vol. 38. Mineralogical Society of America, pp. 1–19.

Gauthier-Lafaye, F., 1986. Les gisements d'uranium du Gabon et les réacteurs d'Oklo. Modèle métallogénique des gites à fortes teneurs du Protérozoïque inférieurs. Mém. Sci. Geol. 78, 206.

Gauthier-Lafaye, F., Weber, F., 1981. Les concentrations uranifères du Francevillien du Gabon: leur association avec des gîtes à hydrocarbures fossiles du Proterozoic inferieur. C. R. Acad. Sci. Paris Ser. II 292, 69–74.

Gauthier-Lafaye, F., Weber, F., 1989. The Francevillian (Lower Proterozoic) uranium ore deposits of Gabon. Econ. Geol. 84, 2267–2285.

Gauthier-Lafaye, F., Holliger, P., Blanc, P.L., 1996. Natural fission reactors in the Franceville basin, Gabon: a review of the conditions and results of a "critical event" in a geologic system. Geochim. Cosmochim. Acta 60 (23), 4831–4852.

Goodarzi, F., Macqueen, R.W., 1990. Optical/compositional character of six bitumen samples from middle Devonian rocks of the Pine Point property, Northwest Territories. Int. J. Coal Geol. 14, 197–316.

Grantham, P.J., Lijmbach, G.W.M., Posthuma, J., Hughes-Clarke, M.W., Willink, R.J., 1988. Origin of crude oils in Oman. J. Pet. Geol. 11, 61–80.

Hidaka, H., Holliger, P., 1998. Geochemical and neutronic characteristics of the natural fossil fission reactors at Oklo and Bangombé, Gabon. Geochim. Cosmochim. Acta 62 (1), 89–108.

Holland, H., 2002. Volcanic gases, black smokers, and the Great Oxidation Event. Geochim. Cosmochim. Acta 66, 3811–3926.

Hunt, J.M., 1995. Petroleum Geochemistry and Geology, second ed. W. H. Freeman & Co., New York, 743 pp.

Huyck, H.L.O., 1990. When is a metalliferous black shale not a black shale? In: Grauch, R.I., Huyck, H.L.O. (Eds.), Metalliferous Black Shales, Related Ore, Deposits, Proceedings, 1989 U.S. Working Group Meeting, International Geological Correlation Program, Project #254, U.S.G.S. Circular 1058, pp. 42–56.

Jackson, S.E., Mossman, D.J., 1999. Quantitative in situ trace element and isotopic analysis of bitumens in ore deposits by laser ablation ICP-MS: a test case. In: Stanley, C.J., et al. (Eds.), Proceedings of the 5th Biennial SGA Meeting and the 10th Quadrennial IAGOD Symposium on Mineral Deposits: Processes to Processing, vol. 1. London, UK, 22–25 August 1999. A.A. Balkema, pp. 231–233.

Jancezek, J., 2000. Mineralogy and geochemistry of natural fission reactors in Gabon. In: Burns, P.C., Finch, R.J. (Eds.), Uranium: Mineralogy Geochemistry and the Environment. Reviews in Mineralogy No. 38. Mineralogical Society of America, pp. 321–392.

Leventhal, J.S., 1993. Metals in black shales. In: Engel, M.H., Macko, S.A. (Eds.), Organic Geochemistry, Principles and Applications. Plenum Press, pp. 581–592.

Leventhal, J.S., 1998. Metal-rich black shales: formation, economic geology and environmental considerations. In: Schieber, J., Zimmerle, W., Sethi, P. (Eds.), Shales and Mudstones II. E. Schweizerbart'sche Verlagsbuchhandlung, Stuttgart, pp. 255–282.

Leventhal, J.S., Giordano, T.H., 2000. The nature and roles of organic matter associated with ores and ore-forming systems: an introduction. In: Giordano, T.H., Kettler, R.M., Wood, S.A. (Eds.), Ore Genesis and Exploration: the Roles of Organic Matter. Reviews in Economic Geology, pp. 1–26.

McKirdy, D.M., Imbus, S.W., 1992. Precambrian petroleum: a decade of changing perceptions. In: Schidlowski, M., Golubic, S., Kimberley, M.M., McKirdy, D.M., Trudinger, P.M. (Eds.), Early Organic Evolution: Implications for Mineral and Energy Resources. Springer-Verlag, pp. 176–192.

Mossman, D.J., 2001. Hydrocarbon Habitat of the Paleoproterozoic Franceville Series, Republic of Gabon. Energy Sources 23 (1), 45–53.

Mossman, D.J., 1998. Hydrocarbon habitat of the Paleoproterozoic Franceville Series, Gabon. In: Mukhopadhyay, P.K., Avery, M.P., Calder, J.H., Goodarzi, F. (Eds.), Abstracts and Program, vol. 15, Annual Meeting of the Society for Organic Petrology. Halifax, Nova Scotia, Canada, p. 15.

Mossman, D.J., Gauthier-Lafaye, F., Jackson, S.E., 2001. Carbonaceous substances associated with the Paleoproterozoic natural nuclear fission reactors of Oklo, Gabon: paragenesis, thermal maturation and carbon isotopic and trace element compositions. Precambrian Res. 106, 135–148.

Mossman, D.J., Jackson, S.E., Gauthier-Lafaye, F., 2000. Nuclear waste disposal—the Oklo analogue. Symposium on Organics in Major Environmental Issues. IGCP Project 429 International Geological Congress, Rio de Janeiro, 7–17 August 2000.

Mossman, D.J., Gauthier-Lafaye, F., Nagy, B., Rigali, M.J., 1998. Geochemistry of organic-rich black shales overlying the natural nuclear fission reactors of Oklo, Republic of Gabon. Energy Sources 20, 521–539.

Mossman, D.J., Nagy, B., 1996. Solid bitumens: an assessment of their characteristics, genesis, and the role in geological processes. Terra Nova 8, 114–128.

Mossman, D.J., Gauthier-Lafaye, F., Nagy, B., Rigali, M.J., 1995. Geochemistry of black shales adjacent the natural nuclear reactors of Oklo, Gabon: the case for hydrothermal alteration. In: Programme with Abstracts, Geological Association of Canada-Mineralogical Association of Canada Annual Meeting, Victoria, British Columbia, 17–19 May 1995, p. A73.

Mossman, D.J., Nagy, B., Rigali, M.J., Gauthier-Lafaye, F., Holliger, P., 1993. Petrography and paragenesis of organic matter associated with the natural fission reactors at Oklo, Republic of Gabon: a preliminary report. Int. J. Coal Geol. 24, 179–194.

Nagy, B., Gauthier-Lafaye, F., Holliger, P., Mossman, D.J., Leventhal, J.S., Rigali, M.J., 1993. Role of organic matter in the Proterozoic Oklo natural fission reactors, Gabon. Geology 21, 655–658.

Nagy, B., Gauthier-Lafaye, F., Holliger, P., Mossman, D.J., Leventhal, J.S., Rigali, M.J., Parnell, J., 1991. Role of organic matter in containment or uranium and fissiogenic isotopes at the Oklo natural reactors. Nature 354, 472–475.

Norman, M.D., Pearson, N.J., Sharma, A., Griffin, W.L., 1996. Quantitative analysis of trace elements in geological materials by laser ablation ICP-MS: instrumental operating conditions and calibration values of NIST glasses. Geostandards Newslett. 20, 247–261.

Parnell, J., Kucha, H., Landais, P., 1993. Bitumen in Ore Deposits. Springer-Verlag, 520 pp. (Special Publication No. 9 of The Society for Geology Applied to Ore Deposits).

Quinby-Hunt, M., Wilde, P., 1991. Provenance of low calcic black shales. Mineralium Deposita 26, 113–123.

Rasmussen, B., Buick, R., 2000. Oily old ores: evidence for hydrothermal petroleum generation in an Archean volcanogenic massive sulfide deposit. Geology 28 (8), 731–734.

Stribrny, B., Urban, H., 1989. Classification of sedimentary rocks in the black shale series based on their normative mineral compositions. In: Proceedings of the 28th International Geological Congress, Washington, DC, pp. 190–191 (Abstracts 3).

Tissot, B., Welte, D., 1984. Petroleum Formation and Occurrence, second ed. Springer-Verlag, 525 pp.

Vine, J.W., Tourtelot, E.B., 1977. Geochemistry of black shale deposits—a summary report. Econ. Geol. 65, 253–272.

Weber, F., 1968. Une série précambrienne du Gabon: le Francevillian. Sédimentologie, géochimie, relations avec les gîtes minéraux associés, Mém. Serv. Carte Géol. Als. Lorr., vol. 28, Strasbourg, 328 pp.

Weber, F., 1973. Genesis and supergene evolution of the Precambrian sedimentary manganese deposit at Moanda (Gabon). In: Proceedings of Kiev Symposium on Unesco, Genesis of Precambrian iron and manganese deposits, 1970, p. 307 (Earth Sciences 9).

Weber, F., 1997. Evolution of lateritic manganese deposits: example of the Moanda sedimentary manganese deposit enriched by lateritization. In: Paquet, H., Clauer, N. (Eds.), Soil and Sediments: Mineralogy and Geochemistry. Springer-Verlag, pp. 97–124.